Magnetic State around Cation Vacancies in II–VI Semiconductors

T. Chanier,[1] I. Opahle,[2] M. Sargolzaei,[2,3] R. Hayn,[1] and M. Lannoo[1]

[1]*Laboratoire Matériaux et Microélectronique de Provence associé au Centre National de la Recherche Scientifique. UMR 6137, Université de Provence, France*

[2]*IFW Dresden, P.O. Box 270116, D-01171 Dresden, Germany*

[3]*Materials Research Laboratory, University of California, Santa Barbara, California 93106, USA*

(Received 26 June 2007; published 17 January 2008)

The magnetic properties of neutral cation vacancies in II–VI semiconductors are examined using first principles calculations and group theory. A molecular cluster model of a single vacancy in II–VI semiconductors is developed to explain the observed chemical trend. We show that a single Zn vacancy in ZnO yields a total spin $S_T = 1$ in agreement with experiments. But for the other less ionic Zn-based II–VI semiconductors ZnA (A = S, Se, Te) this spin triplet state is nearly degenerate with a nonmagnetic spin singlet state.

DOI: 10.1103/PhysRevLett.100.026405 PACS numbers: 71.10.Hf, 71.27.+a, 71.30.+h

The manipulation of the electron spin opens fascinating possibilities for data storage and processing and is conventionally referred to as spintronics [1]. The early results of this research area have already found widespread applications in magnetic hard disk read heads, which use the giant magnetoresistance effect. This new technology has led to a tremendous increase of storage capacity and enabled today's 100-Gbyte disks. For future applications, and especially to solve the problem of effective spin injection, there is a strong demand for new ferromagnetic semiconductor materials with a high Curie temperature. In that respect, defect-mediated ferromagnetism, as, for example, due to vacancies, is intensively discussed [2–6]. A necessary prerequisite for a ferromagnetic state is a local magnetic state around the vacancies. In a more general sense, the investigation of intrinsic point defects in semiconductors, especially in II–VI semiconductors (SC), has already a long history [7–9]. Defects determine in a crucial way their optical, electrical, and growth properties. Surprisingly, despite the enormous literature on that subject, only a few studies deal with the possibility of magnetic states. Magnetic impurity states are also highly interesting candidates for numerous magneto-optical effects and applications, like the so-called spin-LED (light emitting diode) [10].

In this Letter, we present a systematic study of the possible local magnetic order around vacancies in II–VI SC to put earlier discussions on defect-mediated ferromagnetism on a firm basis. In particular, we show that a neutral cation vacancy in II–VI SC favors a magnetic triplet state ($S_T = 1$, two holes with parallel spin), while for an anion vacancy the nonmagnetic spin singlet state is lowest in energy. The energy difference between the singlet and the triplet state around cation vacancies depends strongly on the ionicity of the compound: within the series ZnA (A = O, S, Se, and Te), only ZnO has a well separated magnetic ground state, while for the other less ionic compounds both states are nearly degenerate. We extend the occasional theoretical hints [11] for magnetic states around vacancies in II–VI SC into a systematical investigation of the chemical trend. Our results agree with very early measurements of the $S_T = 1$ state of neutral Zn vacancies in electron irradiated ZnO using electron paramagnetic resonance [12], whereas no indications of such a state seem to be known for ZnSe [13]. The possible existence of a spin triplet state for neutral intrinsic defects has important consequences for magnetic, magneto-optic, or other measurements.

Vacancies in II–VI SC build local defect states and exist in several charge states [9]. The twofold charged vacancies contain no electron or hole in its neighborhood and may not lead to local magnetism. The singly charged vacancies have necessarily an unpaired electron or hole, corresponding to $S_T = 1/2$. The only nontrivial question appears for neutral vacancies, which will be studied below.

We have performed electronic structure calculations in the framework of density functional theory using the supercell approach to study the magnetic properties of vacancies in the II–VI SC ZnA (A = O, S, Se, Te). The calculations were performed with the scalar relativistic version of the full potential local orbital (FPLO) code [14] using the local (spin) density approximation [L(S)DA] in the parametrization of Perdew and Wang [15]. In the FPLO method a minimum basis approach with optimized local orbitals is employed, which allows for accurate and efficient total energy calculations. The convergency of the results with respect to the basis set and k-space integrals (with up to 1728 k points in the full Brillouin zone) was carefully checked. The basis set used for the present calculations consisted of Zn $3spd4spd$, O $2sp3d$, S $3spd$, Se $3d4spd$, and Te $4d5spd$. In addition, empty spheres were included at the vacancy site, which serve together with the other polarization states (Zn $4d$, O $3d$, S $3d$, Se $4d$, and Te $5d$) to improve the completeness of the basis set.

The heavier ZnA compounds ZnTe and ZnSe crystallize in the cubic zinc blende (ZB) structure, while ZnO crystallizes in the wurtzite (W) structure, and ZnS exists in both variants. To distinguish between structural effects and

chemical trends within the series, we performed supercell calculations in both the ZB and W structures. We used supercells with up to $64 = 4 \times 4 \times 4$ atoms in the ZB structure (including the vacancy) or with 16 atoms in the W structure. Finite size effects were estimated by the comparison with smaller 8 atom supercells in the ZB structure, which confirmed the results of the larger cells. The calculations have been performed with the experimental lattice parameters [16–18], and in the case of ZnO in the ZB structure we used lattice constants corresponding to the experimental unit cell volume. We compared calculations without and with lattice relaxation of the vacancy nearest neighbors.

For all compounds of the series, without lattice relaxation, the spin-polarized LSDA total energy is lower than the nonmagnetic LDA one (Table I). This is in agreement with our fixed spin moment calculations showing an energy minimum at the position of the LSDA magnetic moment. However, this minimum becomes more and more shallow with decreasing ionicity going from O to Te. On the other hand, an anion vacancy does not lead to a stable magnetic solution in agreement with earlier studies [9]. Table I shows also the important influence of lattice relaxation on the stability of the magnetic state. Only the vacancy nearest neighbor (NN) anions were allowed to relax while the other ions were fixed at their ideal coordinates. In all cases a compression of the NN tetrahedron was found consistent with simple electrostatic arguments. The calculated values of NN relaxation for $Zn_{31}A_{32}$ (A = O, S, Se, Te) are 9.6%, 10.2%, 7.0%, and 1.2%, respectively. This NN relaxation follows roughly the trend in the ionicity within the series: the charge transfer, calculated for the pure ZnA compounds, reduced from about 1.1 (ZnO) to 0.2 (ZnTe) electrons at the anion site. Existing literature values of the NN relaxation for ZnSe [19] also agree with our results. Finally, we compared the LDA and LSDA energies on the relaxed supercells (Table I). We see that a spin triplet state is stable for the more ionic compound ZnO, for both the relaxed and the unrelaxed cases (ZB and W structures), with an energy gain of at least 70 meV. For the other II–VI SC, the magnetic and nonmagnetic solutions are nearly degenerate for the relaxed case within the precision of our calculations of 1–2 meV.

TABLE I. Total energy difference $\Delta E = E_{\mathrm{LDA}} - E_{\mathrm{LSDA}}$ and LSDA magnetic moments M obtained from unrelaxed and relaxed calculations.

	Unrelaxed		Relaxed	
Supercell	ΔE (meV)	M (μ_B)	ΔE (meV)	M (μ_B)
$Zn_{31}O_{32}$ (ZB)	106.1	2.00	76.2	2.00
$Zn_{31}S_{32}$ (ZB)	39.7	1.96	−2.3	1.96
$Zn_{31}Se_{32}$ (ZB)	11.2	1.60	1.8	1.29
$Zn_{31}Te_{32}$ (ZB)	0.2	0.72	−0.1	0.43
Zn_7O_8 (W)	102.0	1.93	...	...

For a better understanding of the numerical results, we constructed a molecular cluster model and analyzed its lowest eigenstates. The model consists of four sp^3 molecular orbitals, corresponding to the four dangling bonds pointing towards the vacancy site (Fig. 1). The sp^3 orbital at site 1 is expressed as a function of the atomic orbitals, $\psi_1 = (s + p_x + p_y + p_z)/2$, centered at the given site, and the other three molecular orbitals ψ_j ($j = 2, 3, 4$) are given correspondingly. The Hamiltonian to be projected on this basis $H = H_0 + H_{\mathrm{int}}$, consists of the one-particle Hamiltonian H_0 with kinetic energy and the electrostatic potential created by the four ions, and the Coulomb electron-electron interaction H_{int}.

We have to distinguish two different neutral vacancies: (i) the anion (i.e., oxygen) vacancy with two electrons localized on the cation sp^3 dangling bonds and (ii) the cation vacancy with two holes on the anion bonds. To find the two-particle eigenstates we begin by analyzing the noninteracting one-particle Hamiltonian H_0. In order to diagonalize H_0, we use a group theory approach and classify all possible states according to the irreducible representations of the tetrahedral group T_d. From our original basis set, the only nonzero symmetry adapted linear combinations (SALC) of basis functions are those of the irreducible representations A_1 and T_2 of the T_d group:

$$A_1\colon\ v = \frac{1}{2\sqrt{1+3S}}(\psi_1 + \psi_2 + \psi_3 + \psi_4)$$

$$T_2\colon\ t_x = \frac{1}{2\sqrt{1-S}}(\psi_1 + \psi_2 - \psi_3 - \psi_4)$$

$$t_y = \frac{1}{2\sqrt{1-S}}(\psi_1 - \psi_2 - \psi_3 + \psi_4)$$

$$t_z = \frac{1}{2\sqrt{1-S}}(\psi_1 - \psi_2 + \psi_3 - \psi_4),$$

where S is the overlap integral. The transfer term $\langle\psi_i|H_0|\psi_j\rangle = -\beta$ ($i \neq j$) is negative for an anion vacancy (electron picture, $\beta > 0$) and positive for a cation vacancy (hole picture). Then, for an anion vacancy, $E_{A_1} = \langle v|H_0|v\rangle = -3\beta/(1+3S)$ is lower in energy than $E_{T_2} = \langle t_i|H_0|t_i\rangle = \beta/(1-S)$. In the following, we set the energy of the three T_2 states to zero, and the energy of the A_1 state

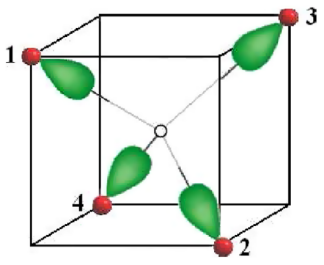

FIG. 1 (color online). Molecular cluster model of the vacancy. The anion and the vacancy are represented by a full and an open circle, respectively, the anion sp^3 hybridization dangling bonds ψ_i are represented in gray (green).

is then given as $\Delta = E_{A_1} - E_{T_2}$. For this case, it can be shown that $S \ll 1$ is a good approximation and leads to $\Delta \approx -4\beta$. For simplicity, the influence of S is neglected below. We have also verified that a small value of S does not change the final conclusions. Figure 2 shows the splitting of hole energy levels due to the tetrahedral symmetry. The value of Δ can be roughly estimated from our band structure results being between 2 and 4 eV. For an anion vacancy (electron picture) the level scheme is simply inverted.

To explain the observed chemical trends, we consider two interacting particles. The two-particle eigenstates are determined by projecting the Hamiltonian on a SALC of two-particle wave functions obtained by group theory. We first determine the representation $T_d \otimes T_d$ and reduce it to irreducible representations. In our basis set, which is composed by products of functions of A_1 (v) and T_2 symmetry (t_x, t_y, t_z), we require only the direct products $A_1 \otimes A_1$, $A_1 \otimes T_2$, and $T_2 \otimes T_2$. Since the character of the direct product representation is equal to the product of the character in each representation the reduction of the representations is obtained by identification: $A_1 \otimes A_1 = A_1$, $A_1 \otimes T_2 = T_2$, and $T_2 \otimes T_2 = A_1 \oplus E \oplus T_1 \oplus T_2$.

The total wave function to be determined here is the product of a spatial wave function and a spin one. For two particles with spin $\frac{1}{2}$, the total spin operator has two eigenvalues, $S_T = 0$ (spin singlet) and $S_T = 1$ (spin triplet). The corresponding spin eigenfunctions are antisymmetric (spin singlet) or symmetric (spin triplet). The spatial wave functions are then constructed such that the total wave function is antisymmetric according to Pauli's principle.

On this symmetry adapted basis set, the Hamiltonian is block diagonal according to group theory. The Coulomb electron interaction is approximately expressed by three parameters, the on-site Coulomb interaction parameter U, the intersite Coulomb parameter V, and the direct exchange parameter J:

$$U = \int d^3r_1 d^3r_2 \frac{\psi_i^2(r_1)\psi_i^2(r_2)}{|r_1 - r_2|},$$

$$V = \int d^3r_1 d^3r_2 \frac{\psi_i^2(r_1)\psi_j^2(r_2)}{|r_1 - r_2|},$$

$$J = \int d^3r_1 d^3r_2 \frac{\psi_i(r_1)\psi_j(r_2)\psi_j(r_1)\psi_i(r_2)}{|r_1 - r_2|},$$

where $i \neq j$. Most blocks are diagonal and the diagonal matrix elements are given in Table II. The only exception is the block of the A_1 representation, which leads to a 2×2 matrix with the off-diagonal term $\sqrt{3}(\frac{1}{4}U - \frac{1}{4}V + \frac{1}{2}J)$. It is easily diagonalized into the corresponding subspace. The results of the molecular cluster model are shown in Fig. 3, as a function of the direct exchange integral J, which has to be positive. The chosen values of U and V for sp^3 orbitals are typical for semiconductors [20], but it should be mentioned that the following conclusions are general and we have verified that they are valid in a very large Δ, U, J, V parameter region.

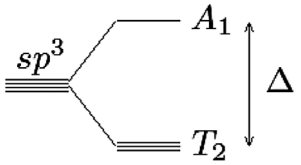

FIG. 2. Hole multiplet splitting for cation vacancy.

The first conclusion to be drawn is the possibility of a magnetic state for a cation vacancy, but not for an anion vacancy. This conclusion is already visible in the one-particle results since two particles in the A_1 state (Fig. 2) prefer to be in the singlet state. On the other hand, two particles in the threefold degenerate state T_2 naturally have the tendency to order their spins in a parallel way according to Hund's rule coupling. We find a threefold degenerate $S_T = 1$ state of T_2 symmetry to be stable for cation vacancies for $J > 0$. For $J = 0$ this state is degenerate with a nonmagnetic $S_T = 0$ state of E symmetry. The energy difference between both states increases proportional to J. This fact explains in part the chemical trend observed in the numerical simulations. Since, in going from O to Te, the lattice constant increases, and also the distance between neighboring sp^3 orbitals, this leads to a decrease of J, which is further reinforced by the stronger screening of the Coulomb repulsion in the more covalent compound ZnTe in comparison to the ionic ZnO [21]. Consequently, the decrease of J leads to less stability of the magnetic $S_T = 1$ state in comparison to the $S_T = 0$ state. The effect of the relaxation is to further lower the energy difference between triplet and singlet states.

The magnetic $S_T = 1$ state around a cation vacancy is found as the ground state in ZnO, which has already been detected experimentally [12]. For the other compounds of the series ZnA (A = S, Se, Te) we found this state to be nearly degenerate with the nonmagnetic one. We suggest that our findings may be extended to all II–VI SC. If we look at the electronegativity difference between group II (Zn, Cd, Hg) and group VI elements, we see that ZnO yields the maximal value of 1.9 eV, compared to the other existing II–VI SC ZnA, CdA, HgA (A = S, Se, Te) with less than 1 eV in Pauling's scale. Therefore it seems that the spin triplet ground state is typical to the more ionic

TABLE II. Classification of two-particle states.

Config.	Spin	State	Deg.	Wave funct.	Diag. term
$v\bar{v}$	0	A_1	1	$v\bar{v}$	$2\Delta + \frac{1}{4}U + \frac{3}{4}V + \frac{3}{2}J$
$t\bar{t}$	0	A_1	1	$x\bar{x} + y\bar{y} + z\bar{z}$	$\frac{3}{4}U + \frac{1}{4}V + \frac{5}{2}J$
$t\bar{t}$	0	E	2	$x\bar{x} - y\bar{y}$	$V + J$
				$2z\bar{z} - x\bar{x} - y\bar{y}$	
$v\bar{t}$	0	T_2	3	$v\bar{x}$, $v\bar{y}$, $v\bar{z}$	$\Delta + \frac{1}{2}U + \frac{1}{2}V$
$t\bar{t}$	0	T_2	3	$x\bar{y}$, $x\bar{z}$, $y\bar{z}$	$\frac{1}{2}U + \frac{1}{2}V - J$
vt	1	T_2	3	vx, vy, vz	$\Delta + V - J$
tt	1	T_2	3	xy, xz, yz	$V - J$

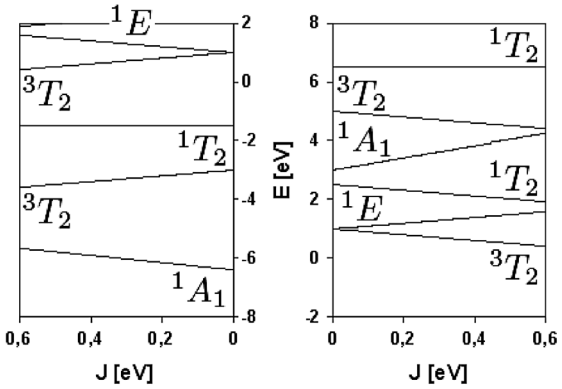

FIG. 3. First low-lying states versus the exchange integral J for anion (left) and cation (right) vacancy. The other parameters are fixed to realistic values: $\Delta = 4$ eV (right) or -4 eV (left), $U = 4$ eV, $V = 1$ eV.

compound ZnO and that the singlet and triplet states are degenerate for most other II–VI SC.

The cation vacancy states act as acceptor impurity levels. Since they are well separated from the valence band edge (by about 0.2–0.5 eV, visible in the band structure), both states are expected to be stable ground (or excited) defect states. Therefore, we speculate that the magnetic state around cation vacancies may also be detected in other II–VI SC. For anion vacancies, our molecular cluster model predicts an excited $^3T_2$ triplet state at about 2.5 eV above the $^1A_1$ singlet ground state (Fig. 3). This was recently observed for oxygen vacancies in ZnO [22].

Around a cation vacancy with cubic symmetry, if the ground state is the partially filled triply degenerate $^3T_2$ state, it should be unstable to a static Jahn-Teller distortion. This implies either a tetrahedral or a trigonal lattice distortion around the vacancy site to lower the energy of the system. This distortion is automatically present in the W structure, but it should appear spontaneously in the ZB structure. Nevertheless, the lattice relaxation [23] is expected to be smaller than the one considered in our study.

Finally, the possibility of long-range ferromagnetic order due to magnetic Zn vacancies can be discussed. It requires a sufficient concentration of vacancies to obtain magnetic percolation, which will probably be different to obtain under equilibrium conditions [3,8]. But even the presence of isolated $S_T = 1$ vacancy states leads to interesting magneto-optic effects or applications. For example, it should be possible to observe magneto-optic dichroism corresponding to transitions between $^3T_2$ and $^1A_1$, which we predict is confined in the visible range.

In this Letter, we investigated the possibility of a magnetic state around cation vacancies in II–VI semiconductors by a combination of *ab initio* and analytical calculations. We showed that the spin triplet state around a Zn vacancy in ZnO is indeed the ground state, in agreement with experiments, and that it is nearly degenerate with the nonmagnetic spin singlet state in other II–VI SC.

Our study was supported by the NATO science division (No. CLG 98 1255), and we thank K. Koepernik and L. Raymond for useful discussions and technical help.

[1] I. Žutić, J. Fabian, and S. D. Sarma, Rev. Mod. Phys. **76**, 323 (2004).
[2] I. S. Elfimov, S. Yunoki, and G. A. Sawatzky, Phys. Rev. Lett. **89**, 216403 (2002).
[3] J. Osorio-Guillén, S. Lany, S. V. Barabash, and A. Zunger, Phys. Rev. Lett. **96**, 107203 (2006).
[4] G. Bouzerar and T. Ziman, Phys. Rev. Lett. **96**, 207602 (2006).
[5] M. Venkatesan, C. B. Fitzgerald, J. G. Lunney, and J. M. D. Coey, Phys. Rev. Lett. **93**, 177206 (2004).
[6] W. Yan, Z. Sun, Q. Liu, Z. Li, Z. Pan, J. Wang, S. Wei, D. Wang, Y. Zhou, and X. Zhang, Appl. Phys. Lett. **91**, 062113 (2007).
[7] F. Rong and G. D. Watkins, Phys. Rev. Lett. **58**, 1486 (1987).
[8] A. F. Kohan, G. Ceder, D. Morgan, and C. G. Van der Walle, Phys. Rev. B **61**, 15019 (2000).
[9] P. Erhart, K. Albe, and A. Klein, Phys. Rev. B **73**, 205203 (2006).
[10] H. J. Zhu, M. Ramsteiner, H. Kostial, M. Wassermeier, H.-P. Schönherr, and K. H. Ploog, Phys. Rev. Lett. **87**, 016601 (2001).
[11] P. Gopal and N. A. Spaldin, Phys. Rev. B **74**, 094418 (2006).
[12] D. Galland and A. Herve, Phys. Lett. **33A**, 1 (1970).
[13] F. C. Rong, W. A. Barry, J. F. Donegan, and G. D. Watkins, Phys. Rev. B **54**, 7779 (1996).
[14] K. Koepernik and H. Eschrig, Phys. Rev. B **59**, 1743 (1999); http://www.FPLO.de.
[15] J. P. Perdew and Y. Wang, Phys. Rev. B **45**, 13244 (1992).
[16] T. M. Sabine and S. Hogg, Acta Crystallogr. B **25**, 2254 (1969).
[17] J. C. Jamieson and H. H. Demarest, J. Phys. Chem. Solids **41**, 963 (1980).
[18] *CRC Handbook of Chemistry and Physics*, edited by R. C. Weast, D. R. Lide, M. J. Astle, and W. H. Beyer (Chemical Rubber, Boca Raton, 1990), 70th ed., pp. E-106 and E-110.
[19] L. Muratov, S. Little, Y. Yang, B. R. Cooper, T. H. Myers, and J. M. Wills, Phys. Rev. B **64**, 035206 (2001).
[20] M. Lannoo and J. Bourgoin, *Point Defects in Semiconductors I, Theoretical Aspects* (Springer-Verlag, Berlin, 1981).
[21] O. Gunnarson, A. V. Postnikov, and O. K. Andersen, Phys. Rev. B **40**, 10407 (1989).
[22] F. H. Leiter, H. R. Alves, A. Hofstaetter, D. M. Hofmann, and B. K. Meyer, Phys. Status Solidi (b) **226**, R4 (2001).
[23] J. Friedel, M. Lannoo, and G. Leman, Phys. Rev. **164**, 1056 (1967).